Magnetic-Shielding Calculations on Al_4^{2-} and Analogues. A New Family of Aromatic Molecules?

Jonas Jusélius, Michal Straka, and Dage Sundholm*

Department of Chemistry, University of Helsinki, P.O. Box 55 (A.I. Virtasen Aukio 1), FIN-00014 Helsinki, Finland

Received: June 19, 2001; In Final Form: September 6, 2001

The molecular structures, the nuclear magnetic shieldings, and the aromatic ring-current shieldings (ARCS) have been calculated for Al_4^{2-}, Al_4Li^-, and Al_4Cu^- at the Hartree−Fock (HF) level, the second-order Møller−Plesset (MP2) level, the coupled-cluster singles and doubles (CCSD) level, and the coupled-cluster singles and doubles level augmented by a perturbative correction for triple excitations (CCSD(T)). The ARCS calculations show that the square-shaped Al_4^{2-} ring sustains a very large diatropic ring current in an external magnetic field. Because the induced ring current is one measure of the molecular aromaticity, the Al_4^{2-} ring can be considered aromatic. Molecular structure optimizations on the group IIIA analogues show that B_4^{2-}, Ga_4^{2-}, In_4^{2-}, and Tl_4^{2-} also exist and have D_{4h} symmetry. The ARCS calculations indicate that they are aromatic, too. New neutral Al_4^{2-} analogues such as Si_2B_2, Si_2Al_2, and Si_2Ga_2 are proposed. The molecular structure and ARCS calculations on the neutral analogues yield planar ring structures with large diatropic ring-current susceptibilities.

1. Introduction

Bimetallic metal clusters consisting of four aluminum atoms and one litium, sodium, or copper atom have recently been studied experimentally with photoelectron spectroscopy.[1] The experimental results were supported by ab initio calculations, which showed that the bimetallic (Al_4M^- with M = Li, Na, or Cu) clusters possess a pyramidal structure of C_{4v} symmetry. The four aluminum atoms form a planar square-shaped ring structure with two delocalized π electrons, suggesting that the aluminum ring, according to the Hückel $(4n + 2)\pi$ rule, is aromatic.[1]

Aromatic compounds are usually described as cyclic molecules with a planar structure, high stability, and large anisotropy in the magnetic susceptibility.[2] The reason for the typical magnetic properties of aromatic molecules is the induced ring current, which today is a generally accepted measure of aromatic character.

In diamagnetic molecules, an external magnetic field induces a current the magnetic field of which lies in the opposite direction to the applied field. In most molecules, this current is located to atoms and chemical bonds, while in cyclic molecules with delocalized π electrons, the induced current is not limited to atoms and bonds. Instead, the external magnetic field creates a ring current, which is much stronger than the induced current of saturated systems.[3−7] The ring current induces a secondary magnetic field perpendicular to the current loop and opposite to the applied magnetic field. In organic molecules, the secondary magnetic field can be experimentally observed as resonance shifts of a few parts per million in the proton magnetic resonance (^{1}H NMR) spectra and computationally as a long-range magnetic shielding. We have recently shown that the strength of the induced ring current or actually the ring-current susceptibility with respect to the strength of the applied magnetic field can be deduced from the long-range behavior of the magnetic shieldings.[8−11]

The aim of this work is to study the molecular structure and the nuclear magnetic shieldings for Al_4^{2-}, Al_4Li^-, and Al_4Cu^- at correlated levels of theory, and to estimate the degree of aromaticity by using the aromatic ring-current shieldings (ARCS) method.[8] The same computational methods are also applied to Al_4^{2-} analogues such as B_4^{2-}, Ga_4^{2-}, In_4^{2-}, and Tl_4^{2-}, as well as to the neutral Si_2B_2, Si_2Al_2, and Si_2Ga_2.

2. Computational Methods

2.1. Al_4^{2-}, Al_4Li^-, and Al_4Cu^-. The molecular structures of the Al_4^{2-} species have been optimized at the self-consistent-field Hartree−Fock (SCF HF) level, the second-order Møller−Plesset (MP2) level, the coupled-cluster singles and doubles level (CCSD),[12] and the coupled-cluster singles and doubles level augmented by a perturbative correction for triple excitations (CCSD(T)).[13,14] The nuclear magnetic resonance (NMR) shieldings have been calculated at the HF,[15] MP2,[16,17] CCSD,[18,19] and CCSD(T)[20] levels of theory using London or gauge-including atomic orbitals (GIAO).[5,15,21,22] In the molecular structure calculations, the core orbitals were frozen, while in the magnetic shielding calculations, all orbitals were correlated.

In the structure calculations, the Karlsruhe triple zeta quality basis sets plus double polarization functions (TZ2P)[23] were employed. For Cu, the valence triple zeta basis set plus double polarization functions (TZV2P) was used.[23] In the magnetic shielding and in the ARCS calculations, the Karlsruhe split-valence basis sets[24] augmented with polarization functions (SVP) as well as the TZ2P (or TZV2P) basis sets were employed. The exponents of the first polarization function were 0.3 (Al), 0.17 (Li), and 0.155 065 (Cu), and the exponents of the second set of polarization functions were 0.52 (Al), 0.1 (Li), and 0.046 199 (Cu). The polarization functions for Li and Cu are of p type,

* To whom correspondence should be addressed. E-mail: sundholm@chem.helsinki.fi (http://www.chem.helsinki.fi/∼sundholm).

10.1021/jp012346h CCC: $20.00 © 2001 American Chemical Society
Published on Web 10/05/2001

and for Al, they are d functions. To check the effect of diffuse basis functions, the aluminum TZ2P basis set was augmented by diffuse basis functions of s, p, and d type (TZ2P+diff). Their exponents were 0.02 (s and p) and 0.06 (d). In the ARCS calculations, the three valence effective core potentials (3-VE ECP) of reference[25] were also employed. The standard ECP basis set was augmented by one diffuse s and p function, two d functions, and one f function. The exponents of the s and p functions were extrapolated from the standard basis set by using the ratio between the two smallest exponents. The exponents of the d functions were taken from reference[26] and the exponent of the f function was 0.2. The ACESII[27] program packages was used.

2.2. B_4^{2-}, Ga_4^{2-}, In_4^{2-}, and Tl_4^{2-}. For B_4^{2-}, Ga_4^{2-}, In_4^{2-}, and Tl_4^{2-}, the molecular structures were optimized at several computational levels using the ACESII,[27] Gaussian 98[28], and Turbomole[29] program packages. For B_4^{2-}, the standard Karlsruhe SVP[24,26] and TZV2P[23] basis sets were employed. For the TZV2P basis set, the exponents of the polarization d functions were 0.29 and 0.87, respectively. For Ga_4^{2-}, the all-electron calculations were performed using the standard Karlsruhe SVP[24,26] basis set and a TZV basis set[23] augmented with two d and one f polarization functions[30] (TZVPP). For Ga_4^{2-}, the molecular structures were also optimized using the three valence electron core potential (3-VE ECP) of reference.[25] For In_4^{2-} and Tl_4^{2-}, we used the Stuttgart 3-VE and 21-VE ECPs[25] in the molecular structure optimizations, while only the 3-VE ECPs were used in the calculation of the magnetic shieldings.

The standard 3-VE ECP basis sets were augmented with diffuse s, p, and d functions as well as an additional set of polarization functions of f type. The exponents of the f functions were 0.309 961 for Ga, 0.2 for In, and 0.2 for Tl. For In and Tl, the standard 21-VE ECP basis sets were augmented by polarization functions of f type. The exponents of the f-type polarization functions were taken from reference 31.

The magnetic shieldings were calculated at the HF (Ga_4^{2-}, In_4^{2-}, and Tl_4^{2-}) and CCSD(T) (B_4^{2-}) levels using ACESII.[27] In the all-electron calculations, GIAO were used, while in the calculations using the ECPs, perturbation-independent basis functions were employed.

2.3. Si_2B_2, Si_2Al_2, and Si_2Ga_2. The molecular structures of the ring-shaped cis and trans isomers of Si_2Al_2 were studied at the HF and CCSD(T) levels using the SVP[24,26] and TZVPP[23,32,33,30] basis sets with two polarization functions of d type and one f function. The Becke three-parameter functional[34] combined with the Lee−Yang−Parr correlation functional[35] (B3LYP) was also used. For the trans isomers of Si_2B_2 and Si_2Ga_2, the molecular structures were optimized only at the HF and B3LYP levels using the SVP and TZ2P basis set. In these calculations, ACESII,[27] Gaussian 98,[28] and Turbomole[29] program packages were used. The magnetic shieldings were calculated at the HF level using GIAOs.

2.4. The ARCS Method. The ring-current susceptibilities (dI/dB) were obtained by performing ARCS calculations. In the ARCS method, the magnetic shieldings are calculated at selected points along a line perpendicular to the molecular plane starting at the center of the molecular ring. The strength of the induced ring current can be estimated by considering the molecular ring as a wire forming a closed circuit. By assuming that the wire carrying the current is circular and infinitely thin, a simple relation between the long-range behavior of the isotropic magnetic shielding function and the current susceptibility with respect to the applied magnetic field can be derived.[8]

TABLE 1: The Bond Lengths (R in pm) for Al_4^{2-}, Al_4Li^-, and Al_4Cu^- Calculated at the HF, MP2, CCSD, and CCSD(T) Levels Using the SVP, the TZ2P (TZV2P for Cu), and the TZ2P+diff Basis Sets as Compared to Previously Calculated Values

molecule	basis sets	level	R(Al−Al)	R(Al−M)[a]	$RR(\perp)$[b]
Al_4^{2-}	TZ2P	HF	258.9		
	TZ2P	MP2	260.0		
	TZ2P	CCSD	257.8		
	TZ2P	CCSD(T)	260.2		
	TZ2P+diff	HF	261.2		
	TZ2P+diff	MP2	261.5		
	TZ2P+diff	CCSD	260.4		
	TZ2P+diff	CCSD(T)	261.8		
	6-311+G*	CCSD(T)	258[c]		
Al_4Li^-	SVP	HF	261.9	304.6	241.8
	SVP	MP2	259.6	288.6	222.7
	SVP	CCSD	258.9	293.7	229.7
	SVP	CCSD(T)	259.7	291.2	226.0
	TZ2P	HF	261.8	301.9	238.5
	TZ2P	MP2	261.9	285.5	217.3
	TZ2P	CCSD	261.2	291.8	225.9
	TZ2P	CCSD(T)	262.4	289.0	221.6
	6-311+G*	CCSD(T)	260[c]	283[c]	215[c]
Al_4Cu^-	SVP	HF	263.4	281.9	211.6
	SVP	MP2	265.7	247.8	161.6
	SVP	CCSD	262.7	258.1	179.2
	SVP	CCSD(T)	264.6	253.5	171.0
	TZ2P	HF	264.0	287.0	218.0
	TZ2P	MP2	268.4	250.3	163.2
	TZ2P	CCSD	265.0	264.0	186.0
	TZ2P	CCSD(T)	267.2	258.5	176.4
	6-311+G*	MP2	269[c]	244[c]	153[c]

[a] M = Li or Cu. [b] The perpendicular distance from the Al_4^{2-} ring to the metal. [c] Reference 1.

The magnetic shielding calculations were performed with the Austin−Mainz version of the ACESII program package.[27] The ring-current susceptibilities were deduced from the magnetic shieldings calculated in the discrete points (dummy atoms) along the symmetry axis using our own software written in Python.[36]

3. Results and Discussions

3.1. Al_4^{2-}, Al_4Li^-, and Al_4Cu^-. The molecular structure calculations show that for Al_4Cu^- the electron correlation effects on the Al−Cu distance (R(Al−Cu)) are much larger than those for R(Al−Al). For R(Al−Al), the basis set quality is as important as the level of correlation treatment. The bond distances are given in Table 1. At the HF level, R(Al−Cu) is 287 pm. The R(Al−Cu) calculated at the MP2 level is only 250 pm, while at the CCSD(T) level, it is 259 pm. These bond distances were obtained using the TZ2P (TZV2P for Cu) basis sets. The corresponding R(Al−Al) values are 264 (HF), 268 (MP2), and 267 pm (CCSD(T)). The bond distances obtained using the SVP basis sets are 1−3 pm shorter. This shows that MP2 is not an appropriate computational level for Al_4Cu^-. Li et al.[1] optimized the structure for Al_4^{2-}, Al_4Li^-, and Al_4Na^- at the CCSD(T) level, while the Al_4Cu^- structure was optimized at the MP2 level. As seen in Table 1, for Al_4^{2-} and Al_4Li^-, there is a relatively good agreement between the present structures and those calculated by Li et al.,[1] while for Al_4Cu^-, they obtained a structure with a significantly shorter Al−Cu distance than that obtained here at the CCSD(T) level. The neutral Al_4Li_2 is found to be a stable bipyramidal molecule with a planar Al_4^{2-} unit surrounded by the two Li^+ cations.

Because electron correlation effects were found to be significant, the nuclear magnetic resonance (NMR) shieldings and the ARCS were studied at correlated levels of theory using

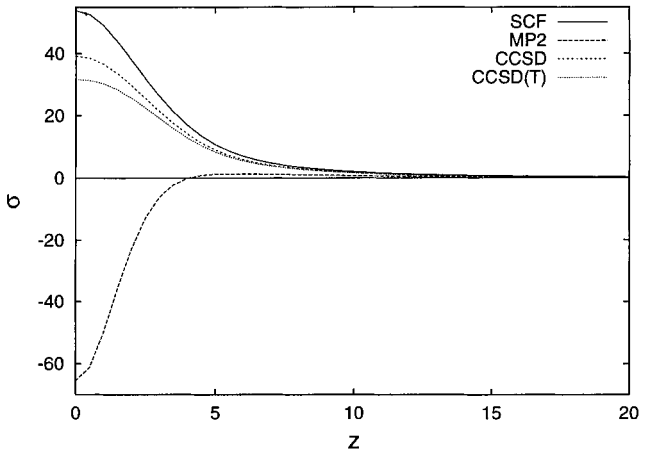

Figure 1. The magnetic shielding as a function of the distance from the center of the Al_4^{2-} ring, calculated at the HF, MP2, CCSD, and CCSD(T) levels using SVP basis sets.

TABLE 2: The Nuclear Magnetic Shieldings (σ in ppm) for Al_4^{2-}, Al_4Li^-, and Al_4Cu^- Calculated at the HF, MP2, CCSD, and CCSD(T) Levels Using the SVP and TZ2P (for Cu TZV2P) Basis Sets

		Al_4^{2-}	Al_4Li^-		Al_4Cu^-	
level	basis	σ(Al)	σ(Al)	σ(Li)	σ(Al)	σ(Cu)
HF	SVP	227.9	80.2	118.3	78.8	3011
MP2	SVP	710.8	495.2	100.2	379.8	2271
CCSD	SVP	324.0	222.5	113.4	206.4	2727
CCSD(T)	SVP	349.1	240.9	112.2	210.4	2708
HF	TZ2P	185.9	24.1	119.2	2.4	2975
MP2	TZ2P	617.8	441.7	100.4	314.7	2213
CCSD	TZ2P	293.8	185.1	113.3		
CCSD(T)	TZ2P	323.8	209.6	111.8		

the SVP as well as the TZ2P (for Cu TZV2P) basis sets. In the shielding calculations, the following bond lengths were adopted. For Al_4^{2-}, the Al−Al distance was taken to be 260.2 pm, for Al_4Li^- the Al−Al distance was 263.0 pm and the Li−Al distance was 289.4 pm, and for Al_4Cu^- the Al−Al distance was 267.2 pm and the Cu−Al distance was 256.1 pm.

The electron correlation effects on the NMR shieldings were found to be very large. For Al_4Li^-, the NMR shielding for aluminum, σ(Al), calculated at the HF level using the TZ2P basis sets is only 24.1 ppm. At MP2 level, the corresponding value is 441.7 ppm. The aluminum shielding obtained at the CCSD and the CCSD(T) level are 185.1 and 209.6 ppm, respectively; thus, the triple contribution to σ(Al) is 24.5 ppm or more than 10% of the total value. The basis set dependence of the NMR shieldings was studied by performing shielding calculations using also the SVP basis sets. As seen in Table 2, the aluminum shielding obtained with the smaller basis sets (SVP) are 30−60 ppm larger than those obtained with the TZ2P basis sets. For σ(Li) and σ(Cu), the basis set effects are small.

The electron correlation contribution to the NMR shieldings calculated at the MP2 level is twice as large as the correlation correction obtained at the CCSD(T) level. However, the electron correlation effect on σ(Li) is small. Because Li in Al_4Li^- formally consists of the Li^+ cation, the triple contribution to σ(Li) is only 1% of the total shielding. However, it is more surprising that the triple contribution to the copper shielding, σ(Cu), in Al_4Cu^- is only 19 ppm or 0.7% of the total copper shielding.

The magnetic shielding functions along the symmetry axis, $\sigma(z)$, calculated for Al_4^{2-} at the HF, MP2, CCSD, and CCSD(T) levels using the SVP basis sets are shown in Figure 1. For small z values, i.e., close to the center of the molecular ring, $\sigma(z)$ depends strongly on the level of correlation treatment. The $\sigma(z)$ calculated at the HF, CCSD, and CCSD(T) levels are similar, but the shielding function calculated at the MP2 level shows the wrong sign at small z values. The nucleus-independent chemical shielding (NICS)[37,38] value calculated at the MP2 level even suggests that the Al_4^{2-} ring would be antiaromatic. The reason for the different behavior at the MP2 level is the important static electron correlation effects.

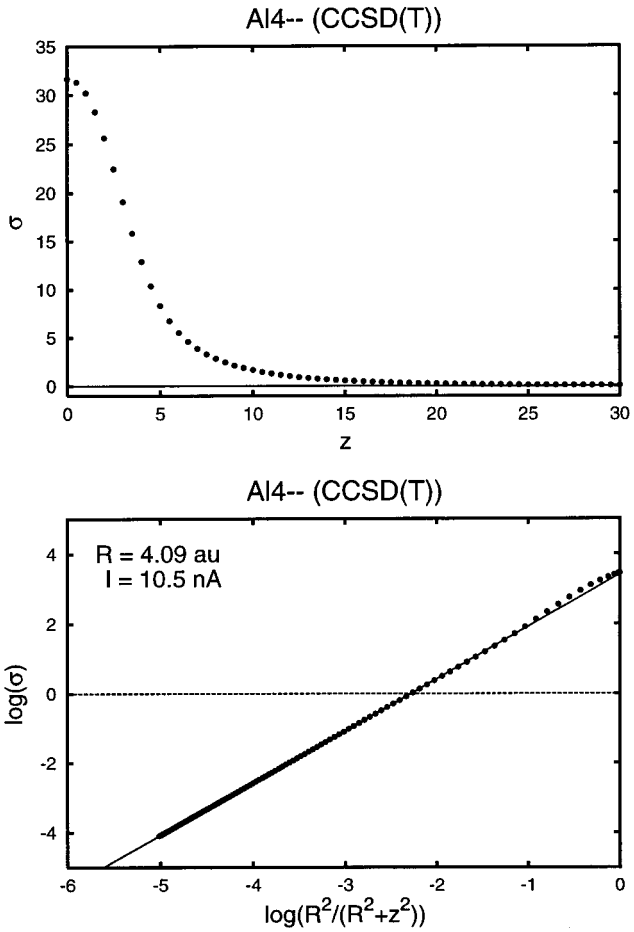

Figure 2. The ARCS plots for the Al_4^{2-} ring calculated at the CCSD(T) level.

By fitting $\sigma(z)$ to an expression derived from Biot−Savart's law for a circular circuit, the ring-current susceptibility and the size of the wire loop can be obtained.[8−11] The ARCS plots for Al_4^{2-} calculated at the CCSD(T) level using the SVP basis sets are shown in Figure 2. The ARCS plots for Al_4Li^- and Al_4Cu^- look very similar. The ARCS plot for Al_4Li^- including the Li atom calculated at the CCSD level is shown in Figure 3. However, a more accurate value for the ring current is obtained when the ARCS shieldings are calculated on the opposite side of the ring. ARCS plots can also be downloaded from our website.[39]

The ring-current susceptibilities and the ring radii (R_{ring}) are given in Table 3. The ARCS calculations show that the Al_4^{2-} ring in Al_4^{2-}, Al_4Li^-, and Al_4Cu^- sustains in magnetic fields a strong diatropic ring current of about 9−12 nA T^{-1}. For comparison, the ring-current susceptibility for benzene is about 8 nA T^{-1}. The ring-current susceptibility for the Al_4^{2-} ring obtained at the HF level is somewhat larger than the coupled cluster values. The ring-current susceptibilities calculated at the MP2 level are not reliable because of the near-degeneration electron correlation effects. This can also be seen from the

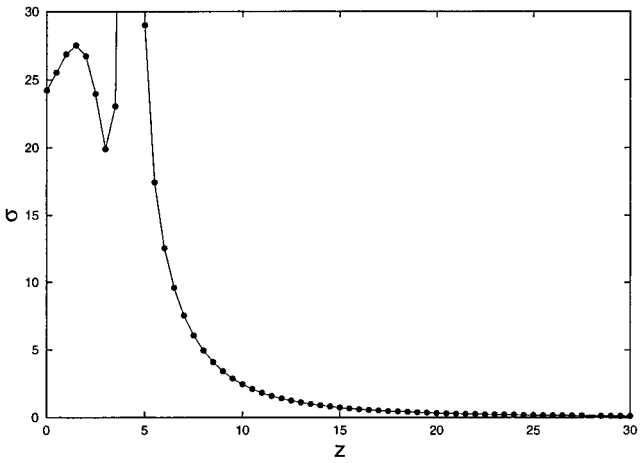

Figure 3. The ARCS plots for Al_4Li^- calculated at the CCSD level. The Li atom is located at 4.19 au from the Al_4^{2-} ring. The NMR shieldings at 4.0 and 4.5 au are 79.3 and 72.9 ppm, respectively.

TABLE 3: The Ring-Current Susceptibility (d*I*/d*B* in nA T^{-1}) and the Radius (R_{ring} in pm) of the Current Loop as Obtained in the Aromatic Ring-Current Shielding Calculations Using the SVP Basis Sets; for Al_4^{2-}, the d*I*/d*B* Obtained in the 3-VE+sp2df ECP Calculations Are Also Given

molecule	level	d*I*/d*B*	R_{ring}
Al_4^{2-}	HF	14.2	204
	MP2	2.0	399
	CCSD	11.6	211
	CCSD(T)	10.5	217
	ECP HF	16.2	194
	ECP CCSD	14.4	195
Al_4Li^-	HF	11.4	226
	MP2	62.1	65
	CCSD	11.9	197
Al_4Cu^-	HF	8.8	265
	MP2	34.8	95
	CCSD(T)	8.1	248

shielding function, $\sigma(z)$, and from the unreasonable ring radii obtained in the ARCS fits. The close agreement between the ring-current susceptibilities obtained at the CCSD and the CCSD(T) levels shows that higher-order correlation contributions are small. The calculations also show that the ring-current susceptibility can be estimated at the HF level even though the electron correlation contribution to the NMR shieldings is large.

3.2. B_4^{2-}, Ga_4^{2-}, In_4^{2-}, and Tl_4^{2-}. Because Li et al.[1] proposed that the Ga_4^{2-}, In_4^{2-}, and Tl_4^{2-} analogues might exist and show aromatic character, these species as well as the related B_4^{2-} were included in our study. The molecular structure optimizations on B_4^{2-}, Ga_4^{2-}, In_4^{2-}, and Tl_4^{2-} calculated at different levels of theory yield molecules of D_{4h} symmetry. The ground-state occupation in D_{4h} symmetry of 14 valence electrons for the B, Ga, In, and Tl analogues was, as for Al_4^{2-}, found to be a_{1g}, e_u, b_{1g}, b_{2g}, a_{1g}, a_{2u}, which corresponds to the $4a_1$, $1a_2$, $1b_1$, $1b_2$ occupation in C_{2v}.

For the Ga analogue, the molecular structure and the vibrational frequencies obtained in the all-electron calculation are compared in Table 4 with the corresponding data of the 3-VE ECP HF calculations. The bond lengths of the ECP calculations are about 3 pm longer than those obtained in the all-electron calculations. In the correlated all-electron calculations on Ga_4^{2-}, the 1s2s2p3s3p core orbitals were frozen. All vibrational frequencies are real showing that the square-shaped Ga_4^{2-} structure is a minimum. As seen in Table 4, the vibrational frequencies are found to be almost independent of the level of calculation.

TABLE 4: The Molecular Structure of Ga_4^{2-} (in pm) and the Harmonic Vibrational Frequencies (in cm^{-1}) Obtained at Different Computational Levels

level	basis set	*R* (pm)	b_{2g}	a_{1g}	e_u	b_{1g}	b_{2u}
HF	3-VE+1d	256.8	209	189	156	99	80
	SVP	255.5	215	201	161	95	80
	3-VE+sp2d1f	258.8	194	181	153	90	75
	TZVPP	255.8	215	199	161	95	79
B3LYP	3-VE+1d	256.5	194	183	164	99	81
	SVP	254.4	198	192	171	98	86
	3-VE+sp2d1f	257.4	184	179	162	90	76
	TZVPP	253.6	199	191	170	100	84
MP2	3-VE+1d	257.3	195	191	200	95	84
	SVP	252.2	206	206	219	98	88
	3-VE+sp2d1f	256.7	190	190	198	84	77
	TZVPP	249.3	217	214	225	104	94
CCSD(T)	3-VE+1d	258.6	195	187	172	90	78
	SVP	254.0	204	201	183	92	78
	3-VE+sp2d1f	257.4	189	185	171	82	73

TABLE 5: The Molecular Structure of B_4^{2-}, In_4^{2-}, and Tl_4^{2-} (in pm) and the Harmonic Vibrational Frequencies (in cm^{-1}) Obtained at Different Computational Levels

molecule	level	*R* (pm)	b_{2g}	a_{1g}	e_u	b_{1g}	b_{2u}
B_4^{2-}	HF TZV2P	164.7	994	904	99*i*	381	401
	B3LYP TZV2P	164.4	942	901	688	408	360
	CCSD(T) TZV2P	166.8	903	881	709	375	286
In_4^{2-}	CCSD(T) 3-VE+1d	298.8	136	126	103	58	44
	HF 3-VE+sp2d1f	296.4	129	122	105	54	45
	B3LYP 3-VE+sp2d1f	294.2	124	121	120	55	46
	MP2 3-VE+sp2d1f	296.1	125	125	129	51	48
	CCSD(T) 3-VE+sp2d1f	297.0	124	122	113	49	44
	B3LYP 21VE+4f	290.8	123	122	112	54	49
Tl_4^{2-}	CCSD(T) 3-VE+1d	305.7	93	86	73	45	37
	HF 3-VE+sp2d1f	306.3	85	79	72	40	35
	B3LYP 3-VE+sp2d1f	304.5	79	78	71	41	35
	MP2 3-VE+sp2d1f	303.8	83	83	81	38	36
	CCSD(T) 3-VE+sp2d1f	304.7	82	81	76	36	34
	B3LYP 21VE+4f	301.8	86	85	80	38	34

For B_4^{2-}, the structure and the vibrational frequencies obtained at the HF, B3LYP, and CCSD(T) levels using the TZV2P basis sets are given in Table 5. At the HF level, two frequencies were imaginary, while at the density-functional and coupled-cluster levels, the square-shaped B_4^{2-} is a minimum on the potential energy surface. To our knowledge, B_4^{2-} is a new boron species.

The molecular structures of the In and Tl analogues were calculated using the 3-VE ECPs as well as the more accurate 21-VE ECPs. For In_4^{2-}, the bond lengths obtained using the 3-VE ECPs are 3−4 pm longer than those obtained with the smaller 21-VE ECP. For Tl_4^{2-}, the 3-VE ECP bond distances are in satisfactory agreement with those obtained with the smaller ECP. The bond lengths vary less than 4 pm depending on the size of the basis sets and the level of correlation. The basis sets are probably not completely saturated, but the usage of still larger basis sets would not change the qualitative picture. The present calculations show that In and Tl analogues may exist. A comparison of the structure and the vibrational frequencies for the B, Ga, In, and Tl analogues shows that the bond lengths increase with increasing nuclear charge and that the force constants decrease. The stability of the systems decreases with increasing nuclear charge.

Relativistic effects are important for the heavier species particularly for Tl_4^{2-}. The spin−orbit coupling effects were not explicitly included in the present study, but scalar relativistic effects are considered by employing relativistic ECPs. For the Tl species, the 6p spin−orbit splitting is probably large and might change the bonding in the molecule, while for the lighter elements, the spin−orbit effects are less significant.

TABLE 6: The Ring-Current Susceptibilities (d*I*/d*B* in nA T^{-1}) and the Ring Radius (R_{ring} in pm) for B_4^{2-}, Ga_4^{2-}, In_4^{2-}, and Tl_4^{2-} as Obtained at Different Computational Levels

molecule	level	structure	basis set	d*I*/d*B*	R_{ring}
B_4^{2-}	HF	SVP CCSD(T)	SVP	7.6	185
	CCSD(T)	SVP CCSD(T)	SVP	7.4	168
Ga_4^{2-}	HF	SVP HF	SVP	13.2	205
	HF	SVP HF	TZVPP	12.2	216
	HF	3-VE+1d HF	3-VE+1d	18.7	199
	HF	3-VE+1d HF	3-VE+sp2df	17.2	190
In_4^{2-}	HF	3-VE+1d HF	3-VE+1d	22.9	209
	HF	3-VE+1d HF	3-VE+sp2df	18.8	209
	HF	3-VE+1d CCSD(T)	3-VE+1d	24.6	205
	HF	3-VE+1d CCSD(T)	3-VE+sp2df	19.3	210
Tl_4^{2-}	HF	3-VE+1d HF	3-VE+1d	22.6	222
	HF	3-VE+1d HF	3-VE+sp2df	18.2	235
	HF	3-VE+1d CCSD(T)	3-VE+1d	23.8	220
	HF	3-VE+1d CCSD(T)	3-VE+sp2df	18.4	241

For the Ga, In, and Tl analogues, the magnetic shieldings were calculated at the HF level, while for B_4^{2-}, the magnetic shieldings were also studied at the CCSD(T) level. In the all-electron calculations, GIAOs were used. With the present version of the ACESII program, GIAOs cannot be used in combination with ECPs. Magnetic shieldings calculated with perturbation-independent basis functions suffer from the well-known gauge problem.[5,15,21,22] A comparison of the magnetic shielding showed that in the 21-VE ECP calculations the uncertainties introduced by gauge problem are too large for a reliable estimation of the ring-current susceptibilities, while in the 3-VE ECP calculations, the basis sets could be augmented so that the errors introduced because of gauge problem became small.

The ring-current susceptibilities for Ga_4^{2-} obtained at the HF level using the large core ECPs (3-VE ECP) are about 30% larger than the values of the all-electron calculation. For the smaller basis sets (3-VE+1d), the obtained ring-current susceptibility is about 10% larger than the 3-VE+sp2df value. This shows that the ring-current susceptibilities can be estimated at the 3-VE+sp2df HF level. As seen in Table 3, for Al_4^{2-}, the 3-VE+sp2df calculations yield ring-current susceptibilities that are 15−25% larger than the corresponding results obtained in the all-electron calculations. The ring-current susceptibilities are summarized in Table 6. For Ga_4^{2-}, In_4^{2-}, and Tl_4^{2-} the susceptibilities are almost equal and somewhat larger than for benzene. For B_4^{2-}, the obtained ring-current susceptibility of 7.4 nA T^{-1} is only 10% smaller than for bezene. These results suggest that B_4^{2-}, Ga_4^{2-}, In_4^{2-}, and Tl_4^{2-} can be considered aromatic.

3.3. Si_2B_2, Si_2Al_2, and Si_2Ga_2. A natural extension of this new family of molecules is neutral molecules. Neutral Al_4^{2-} analogues can be constructed by replacing two of the Al or, more generally, two of the group IIIA elements by two of the group IVA elements. In this work, we have considered the analogues obtained by replacing two group IIIA elements by silicon. For example, by replacing two Al atoms in Al_4^{2-} by silicon, two possible structures can be obtained; the trans (here denoted *t*-Si_2Al_2) or the cis (*c*-Si_2Al_2) isomer. At the CCSD(T) level using the TZVPP basis sets, *c*-Si_2Al_2 is 8.8 kJ mol^{-1} below *t*-Si_2Al_2.

For *t*-Si_2Al_2 and *c*-Si_2Al_2, the molecular structures and the vibrational frequencies were calculated at the HF, B3LYP, and CCSD(T) levels using the SVP and TZVPP basis sets. For the planar *t*-Si_2Al_2 and *c*-Si_2Al_2 isomers, all frequencies were real showing that they are true minima. The bond lengths, bond angles, and vibrational frequencies for the Si_2Al_2 isomers are given in Tables 7 and 8.

TABLE 7: The Bond Lengths (in pm) and Bond Angles (in deg) of *t*-Si_2Al_2, *c*-Si_2Al_2, *t*-Si_2B_2, and *t*-Si_2Ga_2 Calculated at Different Levels

molecule	level	basis	M−M[a]	Si−Si	M−Si	∠[b]
c-Si_2Al_2	CCSD(T)	SVP	259.3	222.8	241.7	85.7
	HF	TZVPP	271.4	215.4	246.6	83.5
	B3LYP	TZVPP	260.2	220.0	242.9	85.2
	CCSD(T)	TZVPP	269.7	216.3	244.5	83.7
t-Si_2Al_2	CCSD(T)	SVP	388.7	279.9	239.5	108.5
	HF	TZVPP	398.8	266.6	239.9	112.5
	B3LYP	TZVPP	390.6	276.1	239.2	109.5
	CCSD(T)	TZVPP	391.3	278.6	240.2	109.2
t-Si_2B_2	HF	TZVPP	288.5	264.2	195.6	95.0
	B3LYP	TZVPP	286.7	264.7	195.1	94.5
t-Si_2Ga_2	HF	TZVPP	399.2	269.8	240.1	111.9
	B3LYP	TZVPP	386.5	282.5	239.4	107.7

[a] M is B, Al, or Ga. [b] For *t*-Si_2Al_2, the bond angle is Al−Si−Al, and for *c*-Si_2Al_2, it is defined as Al−Al−Si.

TABLE 8: The Harmonic Vibrational Frequencies (in cm^{-1}) of *t*-Si_2Al_2, *c*-Si_2Al_2, *t*-Si_2B_2, and *t*-Si_2Ga_2 Obtained at Different Computational Levels

molecule	level	basis	b_{3g}	a_g	b_{1u}	b_{2u}	a_g	b_{3u}
t-Si_2Al_2	CCSD(T)	SVP	424	405	401	314	208	133
	HF	TZVPP	446	416	291	265	240	129
	B3LYP	TZVPP	420	398	376	298	216	132
	CCSD(T)	TZVPP	419	399	397	307	208	130
molecule	level	basis	a_1	a_1	b_2	a_1	b_2	a_2
c-Si_2Al_2	CCSD(T)	SVP	496	394	355	290	143	110
	HF	TZVPP	574	368	286	211	126	103
	B3LYP	TZVPP	506	375	332	275	159	127
	CCSD(T)	TZVPP	494	391	352	286	153	123
t-Si_2B_2	HF	TZVPP	748	701	567	330	256	141
	B3LYP	TZVPP	707	701	626	525	336	270
t-Si_2Ga_2	HF	TZVPP	389	358	224	217	161	108
	B3LYP	TZVPP	361	331	287	252	150	115

Because the vibrational frequencies and the molecular structures for Si_2Al_2 were not sensitive to the level of correlation treatment, *t*-Si_2B_2 and *t*-Si_2Ga_2 were studied only at the HF and the B3LYP levels. The HF and B3LYP calculations show that *t*-Si_2B_2 and *t*-Si_2Ga_2 are planar and stable molecules. The structures and the vibrational frequencies calculated at the HF and the B3LYP levels are given in Table 7. The Si_2B_2, Si_2Al_2, and Si_2Ga_2 molecules studied in this work and other analogues obtained by permuting the group IIIA and group IVA elements are new neutral molecules that, to our knowledge, have not previously been studied either experimentally or computationally.

An interesting Al_4^{2-} analogue is *t*-B_2C_2. However, our calculations on *t*-B_2C_2 yielded a completely different structure with a triplet ground state. *t*-B_2C_2 has two minima with almost identical energies. One minimum corresponds to a short C−C distance, and for the other minimum, the B atoms are close. The optimization starting from the *c*-B_2C_2 isomer results in a ring opening. Al_2C_2 showed similar behavior. All other species considered were triplet-stable.

The ARCS calculations on *t*-Si_2Al_2, *c*-Si_2Al_2, *t*-Si_2B_2, and *t*-Si_2Ga_2 show that a magnetic field induces large diatropic ring currents, and therefore, these molecules can be considered aromatic. The ring-current susceptibilities and the current radius obtained in the ARCS calculations are given in Table 9.

4. Summary

The present computational study shows that the square-shaped Al_4^{2-} ring and the four-membered rings of its analogues sustain

TABLE 9: The Ring-Current Susceptibilities (d*I*/d*B* in nA T^{-1}) and the Ring Radius (R_{ring} in pm) for *c*-Si_2Al_2, *t*-Si_2Al_2, *t*-Si_2B_2, and *t*-Si_2Ga_2 as Obtained at the HF Level Using the TZVPP (TZV2P for B) Basis Sets

molecule	d*I*/d*B*	R_{ring}
c-Si_2Al_2	8.9	186
t-Si_2Al_2	9.9	191
t-Si_2B_2	15.7	154
t-Si_2Ga_2	10.0	193

large diatropic ring currents in an external magnetic field. Because the ring current is a generally accepted criteria for aromaticity, they can be considered aromatic. One must bear in mind that the degree of aromaticity does not have a unique definition and cannot be mesured directly. Molecules sustaining a diatropic ring current in a magnetic field are not necessarily aromatic, but molecules without a ring current are probably neither aromatic nor antiaromatic.

The new Al_4^{2-} analogues such as B_4^{2-}, Si_2B_2, Si_2Al_2, and Si_2Ga_2 proposed here, as well as the Ga_4^{2-}, In_4^{2-}, and Tl_4^{2-} species proposed by Li et al.,[1] are found to be minima on the potential energy surface. All Al_4^{2-} analogues considered in this work are aromatic except C_2B_2. The aromaticity of C_2B_2 was not studied because it has a triplet ground state. Indium and thallium analogues as well as more general neutral Al_4^{2-} analogues obtained by mixing two different elements from group IIIA with one or two different elements from group IVA or vice versa might also exist and show aromatic character, but they have not been studied in this work. Our calculations show that the photoelectron spectroscopy study by Li et al.[1] indeed opened the avenue to a new family of aromatic inorganic compounds.

Since the submission of the manuscript, two related papers have appeared. Li et al.[40] extended their photoelectron spectroscopy study to Al_3Si^-, Al_3Ga^-, Al_3Sn^-, and Al_3Pb^-. They found that this series of molecules have cyclic planar structures and are likely aromatic. Fowler et al.[41] presented current-density maps for Al_4^{2-}, Al_4Li^-, Al_4Na^-, and Al_4Cu^- and concluded that in these molecules the delocalized diatropic ring current is carried by σ and not by π electrons.

Acknowledgment. We thank Prof. J. Gauss for a fresh copy of the Austin−Mainz version of ACESII, Prof. Reinhart Ahlrichs for a modern version of Turbomole, and Dr Henrik Konschin for discussions. The generous support by Prof. P. Pyykkö and by The Academy of Finland is also acknowledged. Computing resources at the Centre for Scientific Computing (CSC) are gratefully acknowledged. We acknowledge the support from the European research training network on "Molecular Properties and Molecular Materials" (MOLPROP), Contract No. HPRN-2000-00013.

References and Notes

(1) Li, X.; Kuznetsov, A. E.; Zhang, H.-F.; Boldyrev, A. I.; Wang, L.-S. *Science* **2001**, *291*, 859.
(2) Lazzeretti, P. *Prog. Nucl. Magn. Res. Spectrosc.* **2000**, *36*, 1.
(3) Badger, G. M. *Aromatic Character and Aromaticity*; Cambridge University Press: New York, 1969.
(4) Lowry, T. H.; Schueller Richardson, K. *Mechanism and Theory in Organic Chemistry*, 2nd ed.; Harper Collins Publishers: New York, 1987.
(5) London, F. *J. Phys. Radium* **1937**, *8*, 397.
(6) Pauling, L. *J. Chem. Phys.* **1936**, *4*, 637.
(7) Fleischer, U.; Kutzelnigg, W.; Lazzeretti, P.; Mühlenkamp, V. *J. Am. Chem. Soc.* **1994**, *116*, 5298.
(8) Jusélius, J.; Sundholm, D. *Phys. Chem. Chem. Phys.* **1999**, *1*, 3429.
(9) Jusélius, J.; Sundholm, D. *Phys. Chem. Chem. Phys.* **2000**, *2*, 2145.
(10) Jusélius, J.; Sundholm, D. *J. Org. Chem.* **2000**, *65*, 5233.
(11) Jusélius, J.; Sundholm, D. *Phys. Chem. Chem. Phys.* **2001**, *3*, 2433.
(12) Purvis, G. D.; Bartlett, R. J. *J. Chem. Phys.* **1982**, *76*, 1910.
(13) Raghavachari, K.; Trucks, G. W.; Pople, J. A.; Head-Gordon, M. *Chem. Phys. Lett.* **1989**, *157*, 479.
(14) Bartlett, R. J.; Watts, J. D.; Kucharski, S. A.; Noga, J. *Chem. Phys. Lett.* **1990**, *165*, 513.
(15) Wolinski, K.; Hinton, J. F.; Pulay, P. *J. Am. Chem. Soc.* **1990**, *112*, 8251.
(16) Gauss, J. *Chem. Phys. Lett.* **1992**, *191*, 614.
(17) Gauss, J. *J. Chem. Phys.* **1993**, *99*, 3629.
(18) Gauss, J.; Stanton, J. F. *J. Chem. Phys.* **1995**, *102*, 251.
(19) Gauss, J.; Stanton, J. F. *J. Chem. Phys.* **1995**, *103*, 3561.
(20) Gauss, J.; Stanton, J. F. *J. Chem. Phys.* **1996**, *104*, 2574.
(21) Hameka, H. *Mol. Phys.* **1958**, *1*, 203.
(22) Ditchfield, R. *Mol. Phys.* **1974**, *27*, 789.
(23) Schäfer, A.; Huber, C.; Ahlrichs, R. *J. Chem. Phys.* **1994**, *100*, 5829.
(24) Schäfer, A.; Horn, H.; Ahlrichs, R. *J. Chem. Phys.* **1992**, *97*, 2571.
(25) Pyykkö, P.; Stoll, H. Relativistic Pseudopotential Calculations, 1993−June 1999. *Chemical Modelling: Applications and Theory*; Specialist Periodical Reports; Royal Society of Chemistry: Cambridge, 2000; pp 239−305.
(26) Huzinaga, S. *Gaussian Basis Sets for Molecular Calculations*; Elsevier: Amsterdam, 1984.
(27) Stanton, J. F.; Gauss, J.; Watts, J. D.; Lauderdale, W. J.; Bartlett, R. J. *Int. J. Quantum Chem., Quantum Chem. Symp.* **1992**, *26*, 879. Stanton, J. F.; Gauss, J.; Watts, J. D.; Lauderdale, W. J.; Bartlett, R. J. ACESII, an ab initio program system includes modified versions of the MOLECULE Gaussian integral program of J. Almlöf and P. R. Taylor, the ABACUS integral derivative program written by T. Helgaker, H. J. Aa. Jensen, P. Jørgensen and P. R. Taylor, and the PROPS property integral code of P. R. Taylor.
(28) Frisch, M. J.; Trucks, G. W.; Schlegel, H. B.; Scuseria, G. E.; Robb, M. A.; Cheeseman, J. R.; Zakrzewski, V. G.; Montgomery, J. A., Jr.; Stratmann, R. E.; Burant, J. C.; Dapprich, S.; Millam, J. M.; Daniels, A. D.; Kudin, K. N.; Strain, M. C.; Farkas, O.; Tomasi, J.; Barone, V.; Cossi, M.; Cammi, R.; Mennucci, B.; Pomelli, C.; Adamo, C.; Clifford, S.; Ochterski, J.; Petersson, G. A.; Ayala, P. Y.; Cui, Q.; Morokuma, K.; Malick, D. K.; Rabuck, A. D.; Raghavachari, K.; Foresman, J. B.; Cioslowski, J.; Ortiz, J. V.; Stefanov, B. B.; Liu, G.; Liashenko, A.; Piskorz, P.; Komaromi, I.; Gomperts, R.; Martin, R. L.; Fox, D. J.; Keith, T.; Al-Laham, M. A.; Peng, C. Y.; Nanayakkara, A.; Gonzalez, C.; Challacombe, M.; Gill, P. M. W.; Johnson, B. G.; Chen, W.; Wong, M. W.; Andres, J. L.; Head-Gordon, M.; Replogle, E. S.; Pople, J. A. *Gaussian 98*, revision A.7; Gaussian, Inc.: Pittsburgh, PA, 1998.
(29) Ahlrichs, R.; Bär, M.; Häser, M.; Horn, H.; Kölmel, C. *Chem. Phys. Lett.* **1989**, *162*, 165.
(30) Wilson, A. K.; Woon, D. E.; Peterson, K. A.; Dunning, T. H., Jr. *J. Chem. Phys.* **1999**, *110*, 7667.
(31) Pyykkö, P.; Straka, M.; Tamm, T. *Phys. Chem. Chem. Phys.* **1999**, *1*, 3441.
(32) Dunning, T. H., Jr. *J. Chem. Phys.* **1989**, *90*, 1007.
(33) Woon, D. E.; Dunning, T. H., Jr. *J. Chem. Phys.* **1993**, *98*, 1358.
(34) Becke, A. D. *J. Chem. Phys.* **1993**, *98*, 5648.
(35) Lee, C.; Yang, W.; Parr, R. G. *Phys. Rev. B* **1988**, *37*, 785.
(36) Python Software Foundation, http://www.python.org/.
(37) von Ragué Schleyer, P.; Maerker, C.; Dransfeld, A.; Jiao, H.; van Eikema Hommes, N. J. R. *J. Am. Chem. Soc.* **1996**, *118*, 6317.
(38) Subramanian, G.; von Ragué Schleyer, P.; Jiao, H., *Angew. Chem., Int. Ed. Engl.* **1996**, *35*, 2638.
(39) Jusélius, J.; Straka, M.; Sundholm, D. http://www.chem.helsinki.fi/~sundholm/qc/al4 arcs.
(40) Li, X.; Zhang, H.-F.; Wang, L.-S.; Kuznetsov, A. E.; Cannon, N. A.; Boldyrev, A. I. *Angew. Chem., Int. Ed.* **2001**, *40*, 1867.
(41) Fowler, P. W.; Havenith, R. W. A.; Steiner, E. *Chem. Phys. Lett.* **2001**, *342*, 85.